Hyperpolarized ^{13}C MR Spectroscopic Imaging: Application to Brain Tumors

I. Park[1,2], P. E. Larson[2], S. Hu[1,2], R. Bok[2], T. Ozawa[3], J. Kurhanewicz[1,2], D. B. Vigneron[1,2], S. R. VandenBerg[3], C. D. James[3], and S. J. Nelson[1,2]

[1]Bioengineering, University of California, San Francisco/Berkeley, San Francisco, CA, United States, [2]Surbeck Laboratory of Advanced Imaging, Department of Radiology and Biomedical Imaging, University of California, San Francisco, San Francisco, CA, United States, [3]Brain Tumor Research Center, Department of Neurological Surgery, University of California, San Francisco, San Francisco, CA, United States

Purpose: Dynamic Nuclear Polarization (DNP) and the recent development of a dissolution process, which retains polarization into the liquid state have enabled the real time investigation of in vivo metabolism with more than 10,000-fold signal increase [1]. The purpose of this study was to explore the feasibility of using ^{13}C MRSI with hyperpolarized $^{13}C_1$-pyruvate as a substrate for evaluation of in vivo brain tumor by comparing hyperpolarized ^{13}C MRSI data from rats with and without intracranial human xenograft tumors. In conducting this study, we characterized and compared ^{13}C imaging parameters with results from histology/immunochemistry for two different tumor types.

Methods: Nine athymic rats with intracranial implantation of human glioblastoma cells (four U-251 MG and five U-87 MG xenograft model) and six normal Sprague-Dawley rats were included in this study. All studies were performed using a GE 3T scanner with a custom-designed ^{1}H/^{13}C rat coil. ^{13}C 2D MRSI (TE/TR=35/110 ms, 10 mm slice centered on brain, 5x5mm in-plane-resolution) was acquired using a double spin echo sequence [2] with a centric k-space encoding and variable flip angle scheme after the injection of 2.3 ml (100mM) hyperpolarized $^{13}C_1$-pyruvate. The animals were euthanized after the experiment, and their brains resected. Proliferation (MIB-1), hypoxia (CA-9) and percent necrosis were evaluated from histology/immunochemistry analysis using previously described methods [3]. The SNR of lactate (Lac), pyruvate (Pyr) and total carbon (tC: a sum of lactate, pyruvate-hydrate, alanine, and pyruvate SNR), as well as the ratio of lactate over pyruvate (Lac/Pyr), lactate over total carbon (lac/tC) and pyruvate over total carbon (Pyr/tC) were calculated from the ^{13}C 2D MRSI magnitude spectra. The carbon spectra were voxel-shifted in order to minimize partial volume effects. All SNR values were normalized according to polarization and injection volume for each exam. To investigate differences between rats with tumor and controls, each ^{13}C MRSI parameter was compared between the voxels containing Gd-enhanced brain tissue in T_1 image of rats with tumors and normal brain tissue in control rats using the Mann-Whitney test. MIB-1 values were compared with the ^{13}C imaging parameters using the Spearman rank correlation.

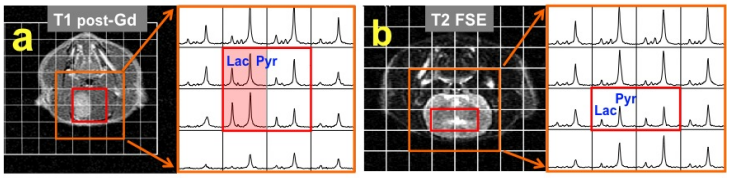

Figure 1: Hyperpolarized ^{13}C MRSI data and the corresponding anatomical images for a tumor (a) and normal rat (b). The lactate and pyruvate levels in the tumor were much higher than those in the brain tissue of the normal rat.

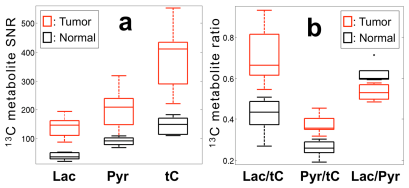

Figure 2: Comparison of the SNR of Lac, Pyr and tC (a) and the ratio of Lac/Pyr, Lac/tC and Pyr/tC (b) between the tumor and normal rats.

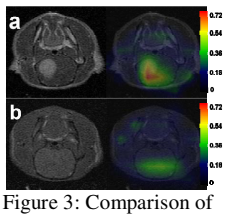

Figure 3: Comparison of Lac/Pyr between a tumor (a) and normal (b) rat.

Results: The ^{13}C lactate and pyruvate data exhibited significantly higher SNR in the tumors compared to normal brain tissue (Figure 1). Statistical analysis showed significant differences in all ^{13}C imaging parameters ($p<0.005$) between tumor and normal brain (Figure 2). In addition to differences between the brains of rats with and without tumor (Figures 1-3), the SNR of Lac, Pyr and tC were significantly different between the brains of rats with U-251 MG and U-87 MG tumors (Figure 4). The histology/immunochemistry also confirmed distinct patterns between the two tumor types (Figure 5). There was significant difference in the percent necrosis ($p<0.02$) and a strong trend toward differences ($p=0.06$) in CA-9 index between U-251 MG and U-87 MG tumors (Table 1). The MIB-1 index (%) and the SNR of Lac appeared to be correlated ($r=0.8$) for each type of tumor; however, the statistical significance of this relationship was limited by the small sample size (Figure 6).

Conclusions: The results of this study revealed significant differences in ^{13}C metabolic characteristics, as indicated by hyperpolarized ^{13}C MRSI data, when comparing tumor and normal brain tissue. Moreover, the SNR of Lac, Pyr and tC were observed to be different between U-251 MG and U-87 MG model, in a manner that was consistent with inherent differences in molecular characteristics between these tumors as supported by the results of immunochemical analysis (Figure 5). Our results suggest that the use of hyperpolarized ^{13}C metabolite imaging may be useful in assessing prognosis and in monitoring response to therapy for brain tumors.

Rat ID	tumor model	MIB-1 (%)	CA-9 (%)	necrosis (%)
BT1	U-251	45.65	10 - 25	≥ 25
BT2	U-251	57.00	10 - 25	≥ 25
BT3	U-251	39.47	10 - 25	≥ 25
BT4	U-251	48.11	≥ 25	≥ 25
BT6	U-87	39.78	0 - 10	none
BT7	U-87	43.65	0 - 10	none
BT9	U-87	48.52	none	0 - 10
BT10	U-87	37.32	0 - 10	none
BT11	U-87	40.04	10 - 25	none

Table 1: Analysis from histology and immunochemistry. Percent necrosis was different between U-251 MG and U-87 MG model ($p<0.02$), while CA-9 showed a strong trend toward difference between two tumor types ($p=0.06$).

References: [1] Golman et al. PNAS, 2006. [2] Cunningham et al. J Magn Reson, 2007. [3] Baia et al. Brain Pathol, 2008.

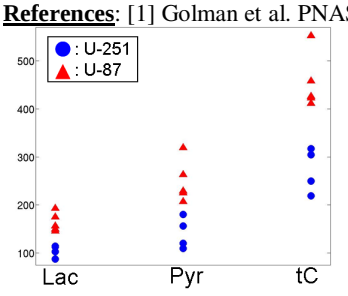

Figure 4: Comparison of the SNR of Lac, Pyr and tC between U-251 MG and U-87 MG xenografts. All three parameters were significantly different between the two tumor types ($p<0.02$).

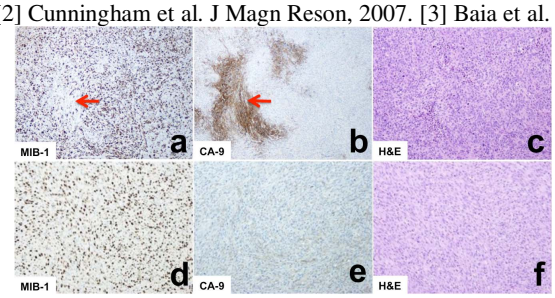

Figure 5: Staining of U-251 MG (a-c) and U-87 MG (d-f) xenografts with MIB-1 (a, d), CA-9 (b, e) and H&E (c, f). In U-251 MG, the zones of cellular hypoxia (arrow in b) corresponded to the zones of lower MIB-1 labeling (arrow in a). In contrast to U-251 MG, the U-87 MG xenografts did not exhibit zonal hypoxia or MIB-1 labeling, and there were no large zones of necrosis.

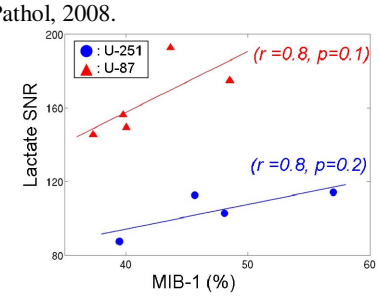

Figure 6: Correlation between the proliferation marker (MIB-1) and the SNR of Lac. Both U-251 MG and U-87 MG xenografts showed strong correlation ($r=0.08$).